Stochastic Techno-Economic Optimization of off-Grid Solar–Wind–Hydrogen–Battery Hybrid Renewable Energy Systems for Rural Electrification Using the Salp Swarm Algorithm

Ganiyu Adedayo Ajenikoko[1], Andrew Oyekanmi Oke[2], Adekunle Sarafadeen Jimoh[3], Abdulbasit Oladayo Ajenikoko[4], Muhammed Daramola Kolapo[5], Israel Damilare Olukotun[6]

[1,2,3,5,6]Department of Electronic and Electrical Engineering
Ladoke Akintola University of Technology
P.M.B, 4000, Ogbomoso, Nigeria.
[4]Department of Electrical and Electronics Engineering
Federal Polytechnic, Ayede, Ogbomoso, Nigeria.
Corresponding Author: ajeedollar@gmail.com
https://doi.org/10.56201/ijcsmt.vol.12.no10.2026.pg167.180

Abstract

Planning dependable off-grid electricity for isolated settlements requires storage technologies capable of responding to both routine renewable fluctuations and prolonged low-generation periods. This study develops a stochastic techno-economic framework for a photovoltaic–wind–battery–hydrogen microgrid optimized using the Salp Swarm Algorithm (SSA). The architecture combines short-duration battery cycling with an electrolyser, hydrogen reservoir and fuel cell for longer-duration supply support. A constructed hourly demand and renewable-resource dataset represents approximately 600 kWh of community electricity use per day. Three planning scenarios, assigned probabilities of 0.60, 0.25 and 0.15, capture ordinary conditions, extended weak-resource episodes and elevated demand. Component capacities are selected to minimize probability-weighted levelized electricity cost while restricting unserved energy to 0.5% in each scenario. The financial assessment assumes a twenty-year project lifetime and an 8% real discount rate. The best feasible hydrogen-assisted design contains 44.4 kW of photovoltaic generation, 182.4 kW of wind capacity, 63.9 kWh of batteries, 154.3 kg of hydrogen storage, a 14.9 kW electrolyser and a 19.9 kW fuel cell. Its estimated net present cost is US$846,684 and its scenario-weighted electricity cost is US$0.394/kWh. Under the same modeled stress conditions, a battery-only alternative requires substantially greater electrochemical storage and reaches US$0.998/kWh. A design optimized only for normal conditions appears cheaper but experiences 8.38% unmet demand in the adverse-resource scenario. The comparisons indicate that long-duration hydrogen storage can provide planning value when multiday shortages dominate the reliability requirement, although its advantages depend strongly on equipment prices and wind quality. Sensitivity tests reveal significant reliability deterioration with moderate resource reductions or demand growth. The contribution is an integrated, reproducible scenario-constrained evaluation approach, not evidence of field performance. Validation with measured weather, demand, component-cost and safety data remains necessary before translating the findings into an investment decision. Further work should evaluate water requirements, electrolyser degradation, hydrogen safety and critical-load service reliability.

Keywords: *Salp Swarm Algorithm; stochastic optimization; rural electrification; solar–wind microgrid; hydrogen energy storage; battery storage; techno-economic analysis.*

1. Introduction

Supplying electricity to isolated settlements requires a system able to withstand both ordinary hourly variations and infrequent periods of sustained renewable-energy scarcity. Central grid extensions may be financially unattractive where communities are distant from transmission infrastructure or initial demand is modest. Meanwhile, diesel-only solutions expose consumers to fuel delivery costs, maintenance interruptions and price uncertainty. Recent access reporting continues to identify major gaps in sub-Saharan Africa (IEA, 2025b, 2026). Decentralized renewable microgrids offer a credible option, but their success depends on sufficient adequacy at a tariff that consumers can support. Photovoltaic modules and wind turbines have complementary but uncertain output patterns. Batteries provide relatively efficient daily cycling, while hydrogen production and reconversion may offer a longer-duration reserve where a multiday deficit would otherwise require a very large battery. Hydrogen incurs important energy-conversion losses, and its equipment, safety and operating requirements are significant. Whether it improves lifetime system economics is consequently an empirical design question that depends on the resources, demand profile and scarcity events at the site, rather than a conclusion that can be assumed from its storage duration. Technology developments reported by the International Energy Agency highlight growing interest in electrolyser and hydrogen applications, but also the limitations imposed by price, deployment maturity and infrastructure (IEA, 2025a). Off-grid capacity planning therefore needs an explicit comparison between storage architectures and a consistent treatment of expected cost and shortage risk. It should not attribute benefits solely to hydrogen when different reliability constraints, renewable capacities or operating conditions are used between alternatives. The present work examines how an SSA-based optimizer can jointly allocate solar generation, wind generation, battery capacity, electrolyser power, stored hydrogen mass and fuel-cell power. Instead of searching against one average year, it evaluates multiple weather-and-demand conditions. The test is structured to show why the least expensive nominal solution can be less dependable than a design that satisfies adequacy requirements separately in each scenario. This motivation draws on the wider literature concerning metaheuristic sizing, hydrogen energy storage and microgrid reliability (Belboul et al., 2024; Hasan et al., 2026). The objectives are to establish coupled electrical and hydrogen mass-balance equations; build a probabilistic scenario set; minimize delivered-electricity cost subject to a specified energy-shortage ceiling; compare hydrogen-assisted and battery-only arrangements; and examine dispatch, optimizer convergence and input sensitivity. The study provides a methodological demonstration using constructed hourly profiles, rather than an assessment of an existing microgrid. Its conclusions are confined to the model assumptions and scenarios disclosed in Sections 3 and 4.

2. Related Works

Research on off-grid hybrid systems increasingly combines renewable generation, storage and optimized dispatch. Belboul et al. (2024) used an improved salp search for photovoltaic, wind, battery and diesel capacity selection, illustrating the relevance of population-based optimization for autonomous supply. Hydrogen-focused studies extend the decision space by linking electrolysers, tanks and reconversion units to the electricity balance. Such coupling is necessary because a large tank adds little resilience if conversion power is insufficient when a long shortage begins. Hassan et al. (2024) investigated hybrid renewable and fuel-cell configurations with hydrogen storage, while Selim et al. (2024) examined sizing alternatives

that incorporate hydrogen pathways. Their studies identify technical and economic trade-offs associated with conversion efficiency, storage duration and installed generation. Reviews of hydrogen energy management similarly emphasize that component sizing cannot be separated from control priorities and the timing of surplus renewable electricity (Sarwar et al., 2024).
Recent investigations have also examined hybrid storage and planning frameworks for remote microgrids (Modu et al., 2024; Mohammed et al., 2026). Reported cost advantages depend on the choice of benchmark, weather assumptions, component price estimates and reliability criterion. Reviews such as Okoroafor et al. (2026) further underscore that algorithm rankings and storage outcomes are not necessarily transferable across climates or tariff structures. A comparison is most informative when each alternative experience precisely the same demand, weather and service constraints. The specific gap addressed here is a transparent scenario-wise assessment in which a single SSA-based procedure is used to examine hydrogen-assisted and battery-only storage under common financial and physical rules. Normal-weather sizing, adverse-resource stress testing and lifetime economic accounting are combined in one framework. The purpose is to identify when long-duration storage changes feasibility or cost, while making no assumption that SSA or hydrogen must outperform every existing alternative.

3. Methodology

3.1 Study design and system configuration

The autonomous system in Figure 1 combines photovoltaic and wind electricity generation with a battery bank, an electrolyser, hydrogen storage and a fuel cell. Renewable generation first meets instantaneous load and charges the battery; further available power may feed the electrolyser. When a shortfall occurs, the battery is discharged within its operating range, followed by fuel-cell reconversion of stored hydrogen. Curtailment and any remaining unmet demand are explicitly recorded. The system boundary covers generation, storage conversion and dispatch, but not detailed local feeder design.

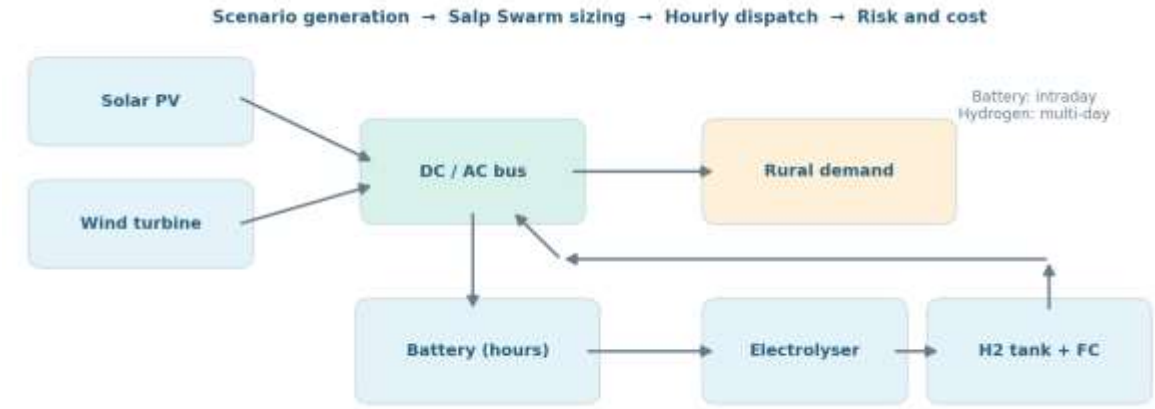


Figure 1. System boundary and energy pathways; conceptual diagram prepared for this article.

3.2 Synthetic demand, renewable data and uncertainty scenarios

A synthetic 365-day hourly series (8,760 steps) was generated using a positive daytime PV shape, a variable wind-capacity-factor series and morning/evening peaks in community load. The unscaled load averages 588 kWh/day, close to a nominal 600 kWh/day. Normal weather has average PV and wind capacity factors of 0.171 and 0.220 respectively. The adverse-resource scenario reduces average resource availability and imposes two prescribed six-to-seven-day low-generation events; the high-demand scenario increases loads by 12%, reduces

average renewable supply modestly and inserts one shorter deficit interval. Scenario probabilities are illustrative planning weights instead of estimated climatological frequencies.

Table 1. Weather-and-demand planning scenarios with assigned probabilities.

Scenario	Weight	PV mean CF	Wind mean CF	Average demand	Stress condition
S1: normal	0.60	0.171	0.220	588 kWh/day	No prolonged forced lull
S2: resource-deficit	0.25	0.146	0.167	594 kWh/day	Two 6–7-day lulls
S3: high demand	0.15	0.163	0.202	659 kWh/day	12% extra load; shorter lull

The scenario-dependent generated power is determined from installed nameplate capacity and dimensionless hourly renewable production factors:

$$P_{RE}(t,s) = C_{PV}\, f_{PV}(t,s) + C_W\, f_W(t,s) \quad (1)$$

The selected stress scenarios deliberately include extended low-generation intervals to test the value of a longer-duration energy reserve. Hourly renewable and load values are retained throughout simulation so that consecutive shortages deplete storage correctly. No claim is made that the scenario probabilities or wind characteristics describe a named Nigerian village; they form a controlled planning dataset that can be replaced by measurements when undertaking a project-specific study.

3.3 Electrical and hydrogen storage equations

For each hour, renewable electricity is used to meet present demand first. Any surplus charges the battery subject to its capacity and charge-power limits; remaining surplus operates the electrolyser and fills the hydrogen tank. During shortfalls, the battery discharges down to its reserve threshold before the fuel cell is dispatched. Unserved energy is recorded only when both sources are insufficient. Charge and discharge variables are non-negative and cannot be active simultaneously.

$$P_{RE} + P_{B,dis} + P_{FC} + P_{UNS} = P_L + P_{B,ch} + P_{EL} + P_{CURT} \quad (2)$$

$$E_B(t+1) = E_B(t) + \eta_{ch}\, P_{B,ch}\, \Delta t - (P_{B,dis}\, \Delta t)/\eta_{dis} \quad (3)$$

$$0.15\, C_B \le E_B(t) \le 0.95\, C_B \; ; \; P_{B,ch}\,, P_{B,dis} \le 0.4\, C_B \quad (4)$$

$$m_{H2}(t+1) = m_{H2}(t) + \eta_{EL}\, P_{EL}\, \Delta t/HHV^* - P_{FC}\, \Delta t/(\eta_{FC}\, HHV^*) \quad (5)$$

$$0 \le m_{H2}(t) \le C_{H2} \; ; \; 0 \le P_{EL} \le C_{EL} \; ; \; 0 \le P_{FC} \le C_{FC} \quad (6)$$

In Equation (5), HHV* is used only as a symbol for the model energy denominator: HHV* = 33.33 kWh/kg is *the lower heating value (LHV)* of hydrogen; the conventional LHV terminology is used throughout the calculations. Electrolyser and fuel-cell efficiencies are 0.65 and 0.51 (LHV basis); battery one-way efficiencies are each 0.94. Thus, the battery round-trip efficiency is approximately 88.4%, whereas the illustrative hydrogen electricity-to-electricity pathway is 33.2% before auxiliary consumption. Compressor energy, start-up

restrictions, part-load efficiency changes, hydrogen leakage and component ageing are outside the simplified dispatch model and must be added in field validation.
Hydrogen and battery inventories begin at 30% and 50% respectively. Terminal inventory requirements allow a maximum 2-percentage-point reduction, limiting the artificial benefit of drawing down initially stored energy without replenishment. Short-term electrical transients and voltage constraints are not simulated; they would require a separate network model.

3.4 Reliability, financing and optimization objectives

Six linked investment decisions are optimized simultaneously: photovoltaic rating, wind rating, battery energy rating, hydrogen storage capacity, electrolyser input power and fuel-cell output power. Because these variables determine how surplus energy is stored and how shortages are supplied, they are evaluated through the same chronological electrical and hydrogen balances.

$$x = [C_{PV}, C_W, C_B, C_{H2}, C_{EL}, C_{FC}] \quad (7)$$

Energy not served (ENS) and the energy-based loss-of-power-supply fraction are calculated for every scenario instead of for the average year alone. The microgrid must satisfy the 0.5% limit separately in all three scenarios.

$$LPSP_s = \Sigma_t P_{UNS}(t,s)\Delta t / \Sigma_t P_L(t,s)\Delta t \leq 0.005 \quad (8)$$

Financial evaluation extends over 20 years with an 8% real discount rate. Initial equipment cost, annual operations and maintenance, and designated replacement expenditures are discounted to obtain net present cost. Figures are calculated in constant US dollars and exclude detailed project financing, taxation and any terminal salvage credit. The same assumptions are applied to all configurations so that the relative comparisons remain consistent.

$$NPC(x) = C_{initial} + \Sigma_y C_{O\&M}/(1+r)^y + \Sigma_k C_{repl,k}/(1+r)^{(y_k)} \quad (9)$$

$$CRF(r,N) = r(1+r)^N / [(1+r)^N - 1] \quad (10)$$

$$LCOE(x) = NPC(x) \cdot CRF(r,N) / \Sigma_s p_s E_{served,s} \quad (11)$$

The objective is the scenario-probability-weighted cost per kilowatt-hour actually served. Shortage constraints are imposed separately for each scenario, together with a terminal-storage consistency requirement. Constraint violations are penalized during search; feasible solutions are then compared using the same underlying life-cycle cost and delivered-energy accounting. This prevents a low-cost configuration from qualifying merely because satisfactory conditions dominate the probability-weighted average.

$$\min_x F(x) = LCOE(x) + 500 \Sigma_s \max(0, LPSP_s - 0.005) + 4 \Sigma_s p_s V_{cyc,s} \quad (12)$$

Here $V_{cyc,s}$ is the dimensionless terminal-inventory violation. It is a numerical penalty instead of an economic cost. The $/kWh interpretation applies to the LCOE term alone. Bounds were PV 20–450 kW, wind 0–220 kW, battery 60–5,200 kWh, hydrogen tank 0–220 kg, electrolyser 0–140 kW and fuel cell 0–110 kW.

Table 2. Synthetic unit financial and technical parameters for the 20-year calculation.

Component	Installed-unit cost	Annual O&M/unit	Planned replacement
Solar PV	$960/kW	$16/kW-year	None
Wind	$1,750/kW	$42/kW-year	None
Battery	$310/kWh	$7.5/kWh-year	Year 10 (77% unit cost)
Hydrogen tank	$1,450/kg	$12/kg-year	None
Electrolyser	$850/kW	$22/kW-year	Year 12 (77% unit cost)

Component	Installed-unit cost	Annual O&M/unit	Planned replacement
Fuel cell	$1,450/kW	$28/kW-year	Year 10 (77% unit cost)

An additional 10% of direct equipment cost represents simplified installation and balance-of-system expenditure. These values are assumed for numerical exploration, not supplier quotations; particularly for electrolysers, real delivered costs may be substantially different (IEA, 2025).

3.5 Salp Swarm Algorithm and comparative experiments

SSA searches the feasible design domain with a leader–follower population. The leading salp is updated relative to the best solution found, and followers move toward neighboring candidates. A decreasing exploration factor progressively changes the balance between searching broadly and exploiting promising regions. Trial capacities are projected onto their allowed bounds, while simulated reliability and terminal-inventory violations are handled through the fitness penalty.

$$x_{(1,j)} = F_j \pm c1[(u_j - l_j)c2 + l_j] \; ; \; c1 = 2\exp[-(4i/I)^2] \quad (13)$$

$$x_{(k,j)} = (x_{(k,j)} + x_{(k-1,j)})/2 \; , \; k \geq 2 \quad (14)$$

In Equation (13), F_j is the jth coordinate of the current best candidate, c2 is uniformly distributed on [0,1], the sign is selected randomly, and I is the maximum iteration count. The implementation uses 34 candidates, 110 iterations and four random seeds for the hydrogen-assisted case; three seeds are used for the battery-only and normal-year alternatives. Following the original SSA framework (Mirjalili et al., 2017), the best solution is preserved after every iteration. Objective and reliability values are recomputed using the same synthetic scenarios for all designs. A battery-only experiment applies exactly the same demand and weather scenarios but forces the hydrogen tank, electrolyser and fuel-cell capacities to zero. A separate arrangement is optimized solely for S1 and then subjected unchanged to S2 and S3. Finally, the specified fixed-capacity battery reference is evaluated using 340 kW photovoltaic generation, 75 kW wind generation and 1,100 kWh of batteries. These tests compare design choices under shared modelling assumptions; they do not establish that SSA is generally superior to alternative solvers.

4. Results and Discussions

4.1 Optimized hybrid microgrid and economic outcome

The feasible hydrogen-assisted solution in Table 3 includes 44.4 kW PV, 182.4 kW wind, 63.9 kWh of batteries, 154.3 kg hydrogen storage, a 14.9 kW electrolyser and a 19.9 kW fuel cell. Estimated installed capital reaches US$711,658; total net present cost is US$846,684 and scenario-weighted LCOE is US$0.394/kWh. In contrast, the battery-only solution meeting the same shortage criteria requires approximately 2,080 kWh of batteries and attains US$0.998/kWh. The resulting 60.5% cost difference reflects the assumed strong wind resource, imposed multi-day deficits and component prices. It should not be generalized to communities with different conditions.

Table 3. Computed system configurations; NPC and LCOE calculated from the stated financial model.

Indicator	Robust battery + H2	Robust battery only	Normal-year SSA
PV capacity (kW)	44.4	446.6	72.5
Wind capacity (kW)	182.4	218.2	88.8
Battery storage (kWh)	63.9	2,080.0	213.0
Hydrogen tank (kg)	154.3	0	~0
Electrolyser (kW)	14.9	0	~0
Fuel cell (kW)	19.9	0	1.2
Installed cost (US$)	$711,658	$1,600,815	$322,474
NPC (US$)	$846,684	$2,144,062	$410,799
Weighted LCOE (US$/kWh)	$0.394	$0.998	$0.197

A major determinant of the solution is the annual wind capacity factor of approximately 0.220 in the ordinary-resource scenario. This favors a sizeable wind installation and alters the relative requirement for battery and hydrogen storage. The selected battery handles daily mismatches, while hydrogen mainly supports more exceptional supply gaps. Wind availability of this quality must be verified locally before investment. Moreover, the financial model does not resolve the full commercial and logistical consequences of hydrogen procurement, safety infrastructure or specialist maintenance in an isolated settlement.

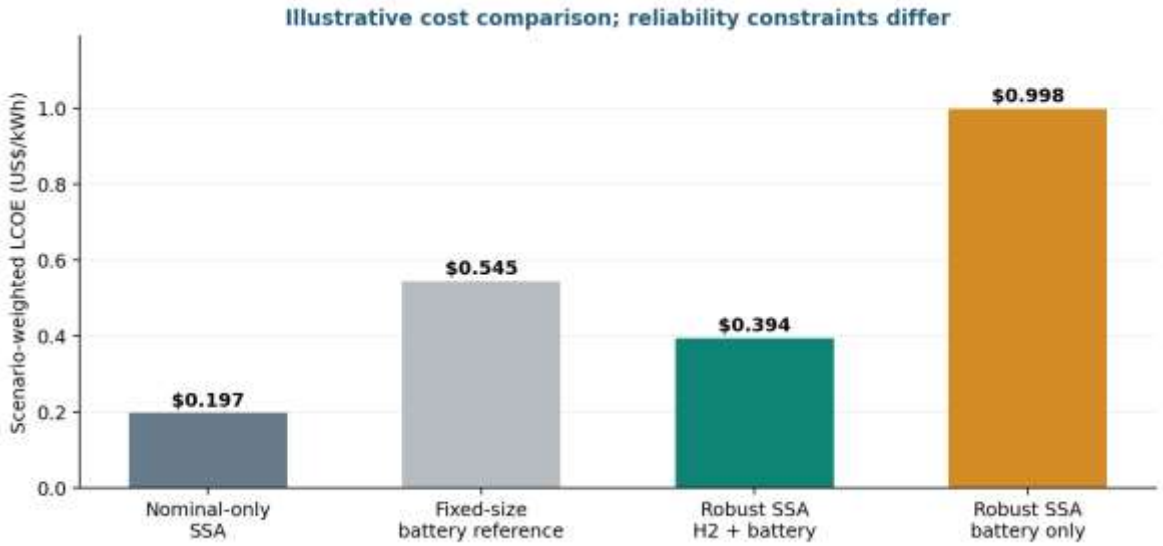


Figure 2. Scenario-weighted electricity cost. The nominal-year and fixed designs violate the stress-scenario reliability threshold.

4.2 Energy adequacy across weather and demand scenarios

The scenario-wise shortage results show that the selected hydrogen–battery system meets the 0.5% limit in all three conditions: approximately 0.000% unserved energy in S1, 0.500% in S2 and 0.010% in S3. The battery-only optimizer also meets the stated limit, with 0.000%, 0.500% and 0.000%, respectively. By contrast, the normal-year-only design faces 8.38% shortages in S2 and 5.26% in S3, notwithstanding its apparent US$0.197/kWh normal-condition cost. Even the fixed reference breaches the S2 threshold at 1.98%. Both feasible optimized designs therefore have little spare margin in the adverse scenario.

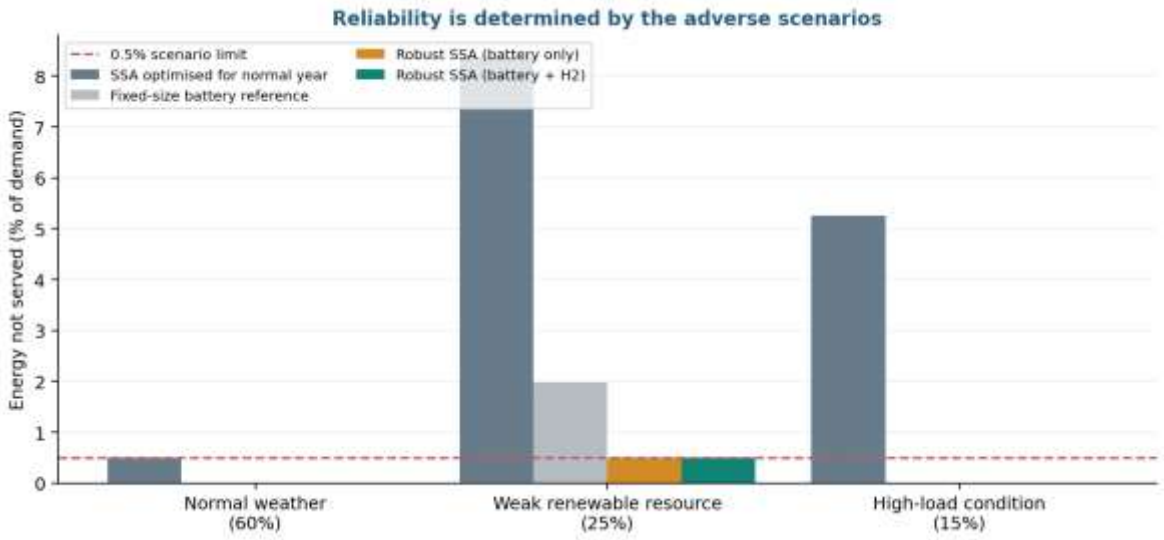


Figure 3. Worst-case adequacy comparison for the three synthetic resource-demand conditions.

The results underscore that positive annual energy production does not guarantee uninterrupted supply. Chronological shortages occurring on consecutive days can exhaust stored energy even when average renewable production exceeds demand. The energy-based LPSP metric also treats all unserved kilowatt-hours equivalently, although a water pump or clinic may require a far higher priority than a deferrable household load. Any field-oriented extension should use critical-load categories and supplement annual shortage fractions with outage frequency, duration and maximum consecutive unmet hours.

4.3 Battery–hydrogen coordination and long-duration storage

The hydrogen trajectory in Figure 4 falls sharply during the first imposed seven-day resource deficit, as the battery supplies only short-term flexibility and the fuel cell covers longer residual shortages. When surplus renewable electricity returns, the electrolyser progressively replenishes stored hydrogen. In the adverse-resource year, cumulative hydrogen throughput is approximately 436 kg, although the maximum tank inventory is only 154.3 kg; cumulative throughput and instantaneous inventory must not be confused. Under ordinary conditions, the modeled throughput is approximately 7 kg, highlighting the role of hydrogen as infrequently used contingency storage.

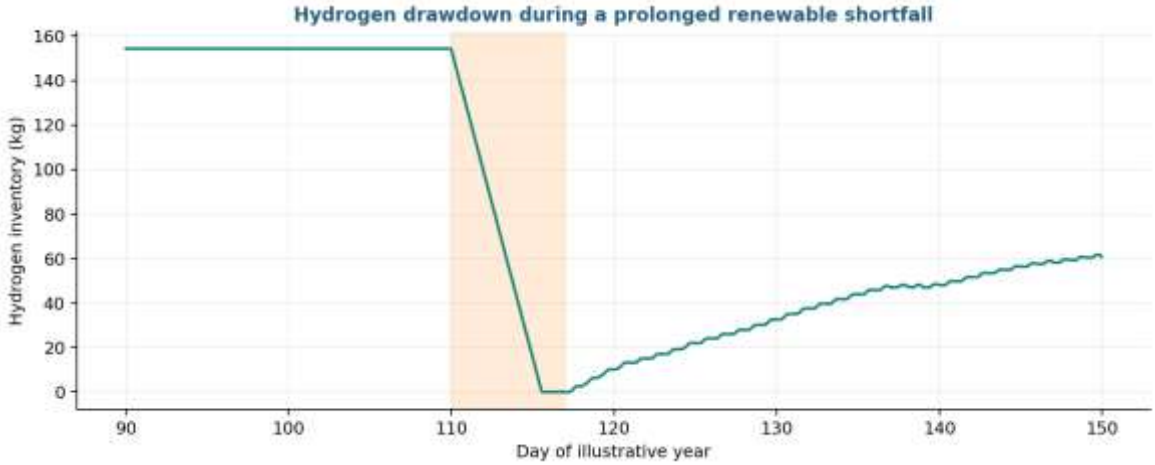


Figure 4. Modeled hydrogen-tank inventory through the first seven-day low-generation interval.

The assumed battery charge–discharge pathway returns approximately 88% of stored electrical energy, compared with approximately 33% for the full electricity–hydrogen–electricity route before auxiliary consumption. The model accordingly gives priority to battery operation during routine imbalances. Hydrogen remains relevant when insufficient long-duration storage would otherwise create significant shortages. Predictive dispatch may improve this trade-off further, but any such benefit should be tested through explicit forecasts and a matched control-policy comparison.

4.4 Convergence, robustness and design sensitivity

The convergence results in Figure 5 show improvement in the SSA-based objective across successive iterations. The lowest feasible weighted LCOE is approximately US$0.394/kWh, while the four repeated hydrogen-assisted runs span roughly US$0.394–0.420/kWh. Such variation confirms sensitivity to initialization and does not establish global optimality. A more rigorous solver assessment should include larger independent samples, comparable function-evaluation budgets and benchmarks against both additional heuristics and mathematical optimization baselines.

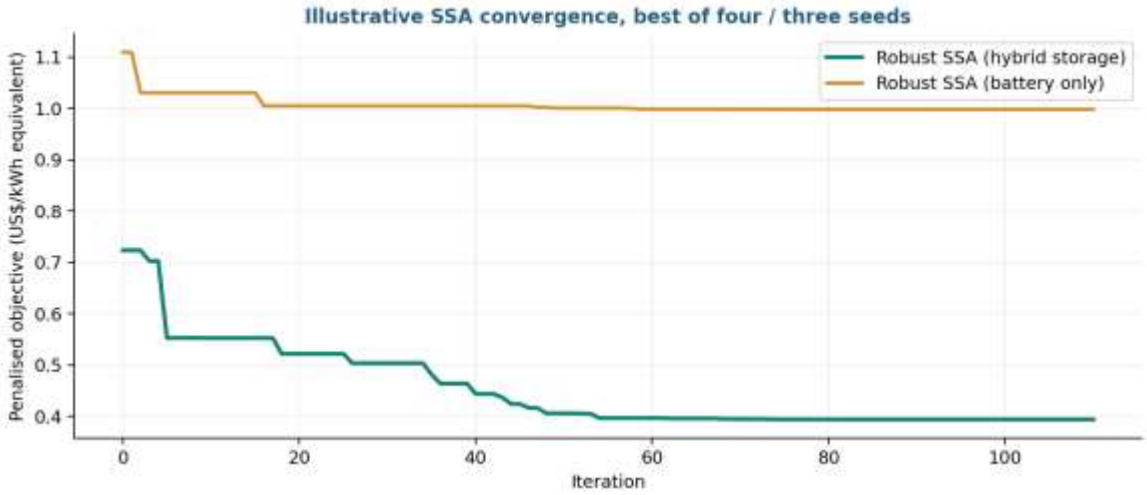


Figure 5. Best-so-far SSA objective values; four independent seeded runs.

One-factor stress testing changes model inputs while holding the chosen equipment capacities fixed. A 10% reduction in wind generation increases the maximum scenario shortage to 2.09%, whereas 10% higher demand increases it to 2.53%. Reducing solar production by 10% raises the shortage fraction to 0.67%. Each perturbation breaches the original 0.5% threshold. Increasing the real discount rate from 8% to 10% instead changes the financial result, raising modeled LCOE from US$0.394 to approximately US$0.445/kWh without affecting physical dispatch. Feasibility should therefore be understood as conditional on the modeled scenario set.

Table 4. One-factor sensitivity of the fixed hybrid design. Changed annual served energy also affects the LCOE denominator.

Test condition	LCOE (US$/kWh)	Worst-scenario unmet energy	Meets 0.5% limit?
Base case	0.394	0.500%	Yes (boundary)
Solar resource −10%	0.394	0.667%	No
Wind resource −10%	0.396	2.090%	No
Demand +10%	0.361	2.527%	No
Wind resource +10%	0.394	0.458%	Yes
Real discount rate 10%	0.445	0.500%	Yes (boundary)

The apparent fall in LCOE when demand increases is not an improvement in service quality. In the present cost-per-served-kWh definition, more energy can be delivered at unchanged capital cost even as the fraction left unserved deteriorates. This is why cost and reliability must always be reported together; for stricter investment appraisal, costs of lost load or explicit critical-service penalties would also be required.

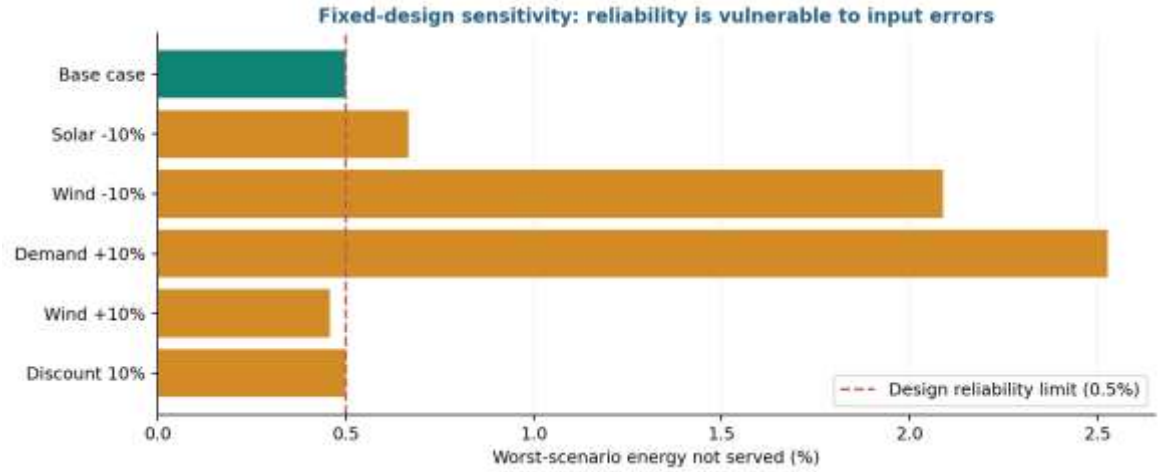


Figure 6. Worst-case reliability deterioration under fixed-design parameter perturbations.

4.5 Implications for rural implementation and limitations

Hydrogen-assisted storage merits closer study when a settlement faces prolonged low-resource periods that make battery-only reserves expensive. Nevertheless, the model output cannot serve as a procurement recommendation. An actual feasibility assessment would need measured demand, multi-season weather observations, vendor quotations, reliable water supply and treatment for electrolysis, hydrogen storage safety design, specialized maintenance arrangements and tariff affordability analysis. Compression energy, conversion degradation, electrical network losses, installation logistics and life-cycle emissions remain outside this simplified model and may materially alter design choices.

The three modeled scenarios deliberately test difficult operating conditions but are not statistically calibrated to a specific climate record. The next research stage should estimate their frequency from observed weather data and challenge the selected configuration with separate out-of-sample years. Feeder load flow, voltage control, hydrogen safety requirements, black-start performance and the cost of interrupted critical supply should be

examined before describing the architecture as technically or financially viable for a particular community.

5. Conclusions

The study establishes an SSA-based planning procedure for a stand-alone photovoltaic–wind microgrid combining batteries and hydrogen storage. An hourly electricity and hydrogen mass balance links generation sizing, electrolyser operation, tank inventory and fuel-cell dispatch to cost and service quality. Three weighted resource–demand scenarios are evaluated with an energy-shortage ceiling enforced independently in each scenario. This avoids accepting a nominally low-cost solution whose deficiencies emerge only during extended renewable shortages. Within the constructed numerical case, the lowest-cost feasible hydrogen-assisted configuration requires 44.4 kW of PV, 182.4 kW wind, 63.9 kWh of batteries, 154.3 kg hydrogen storage, a 14.9 kW electrolyser and a 19.9 kW fuel cell. The resulting net present cost is approximately US$0.847 million and expected unit electricity cost is US$0.394/kWh. Under equivalent assumptions, an admissible battery-only option costs US$0.998/kWh because it requires approximately 2,080 kWh of storage. This contrast illustrates the possible system value of longer-duration reserves for a case containing prolonged generation deficits, rather than a universal cost advantage of hydrogen.

Although the normal-year solution reaches an attractive cost near US$0.197/kWh, its maximum energy shortage increases to 8.38% when tested under adverse resources. The scenario-constrained hydrogen design remains within 0.5% for the conditions used in optimization, but modest declines in wind production or growth in demand cause the fixed design to violate that limit. A system adequate for the assumed scenario set is therefore not automatically resilient to every future climate or consumption pattern.

Storage coordination is crucial. Batteries provide higher-efficiency daily energy shifting, whereas hydrogen can supply comparatively infrequent multiday shortfalls at lower round-trip efficiency. The model's SSA search identifies feasible equipment combinations, but the limited number of independent trials does not justify broad claims of solver superiority. The preferred storage strategy is also sensitive to the assumed resource distribution, conversion losses and technology prices. Future validation should substitute site-monitored solar, wind and consumption records for generated profiles and use quotations that include transport, installation and safety provisions. Long-term degradation, credible climate uncertainty, community critical-load priorities and probabilistic adequacy criteria should be evaluated. Distribution power flow and protection, black start and customer affordability must also be assessed before a deployment decision can be supported by the optimization results.

6. Contribution to Knowledge

The study's principal contribution is the joint treatment of component sizing, chronological energy conversion, multi-scenario reliability and lifetime cost in one traceable methodology. It does not claim to originate SSA, hydrogen technology or stochastic planning. Its value lies in a consistent calculation structure designed to reveal how storage duration and resource uncertainty affect the feasibility of off-grid electrification alternatives.

6.1 Coupled sizing of generation, short-term and long-term storage

The capacity vector includes photovoltaic generation, wind generation, a short-duration battery, electrolyser power, hydrogen reservoir mass and fuel-cell output. Optimizing these jointly prevents a tank-size decision from being separated from the electrical power required to fill or discharge it. The formulation provides a foundation for more detailed equipment efficiency curves, discrete procurement options and location-specific capital costs.

6.2 Explicit scenario-wise energy adequacy

Rather than controlling only average unserved energy, the method enforces an adequacy limit for every stated weather–demand condition. This guards against acceptable performance in frequent ordinary years masking poor service during less frequent extended shortages. The framework could subsequently be expanded to risk-weighted measures, chance constraints or differentiated critical-load reliability requirements.

6.3 Reproducible demonstration of the cost–reliability trade-off

The hydrogen-assisted, battery-only, normal-year and fixed-size references are evaluated using consistent financial and hourly physical assumptions. Their comparison isolates how the available storage options and planning constraints influence cost and supply adequacy. It also demonstrates that reporting LCOE independently of unmet demand can favor an architecture unable to meet a community's service target.

6.4 Separation of calculated outcomes and external evidence

The computational formulation is documented sufficiently to distinguish input assumptions, model calculations and independently published evidence. Capacity allocations, costs and sensitivity values are outcomes of the specified numerical experiments, not field observations. This separation supports independent replication and the eventual replacement of generated inputs with actual weather records, community load surveys and equipment quotations.

6.5 Practical pathway toward decision support

The framework offers a staged route from preliminary screening to practical feasibility: establish critical loads and expected growth, document local resources, obtain market quotations, define credible weather scenarios, optimize capacity and dispatch together, and verify the outcome against unseen conditions. The sensitivity results emphasize the value of reserve margins and alternative supply arrangements whenever a proposed configuration operates close to its reliability ceiling.

References

Belboul, Z., Toual, B., Bensalem, A., Ghenai, C., Khan, B., & Kamel, S. (2024). Techno-economic optimization for isolated hybrid PV/wind/battery/diesel generator microgrid using improved salp swarm algorithm. Scientific Reports, 14, 2920. https://doi.org/10.1038/s41598-024-52232-y

Güven, A. F. (2025). A novel hybrid Salp Swarm Kepler optimization for optimal sizing and energy management of renewable microgrids with EV integration. Energy, 334, 137696. https://doi.org/10.1016/j.energy.2025.137696

Hasan, T., Das, P., Ali, M. F., Alam, M. S., Ali, M., & Imran, I. H. (2026). Techno-economic assessment of a hydrogen-assisted hybrid renewable microgrid with fuel cells for off-grid electrification. Global Challenges, 10(6), e70122. https://doi.org/10.1002/gch2.70122

Hassan, M. H., Kamel, S., Safaraliev, M., & Kokin, S. (2024). Improved techno-economic optimization of hybrid solar/wind/fuel cell/diesel systems with hydrogen energy storage. International Journal of Hydrogen Energy, 68, 998–1018. https://doi.org/10.1016/j.ijhydene.2024.04.124

International Energy Agency. (2025a). Global hydrogen review 2025. IEA. https://www.iea.org/reports/global-hydrogen-review-2025

International Energy Agency. (2025b). Tracking SDG7: The energy progress report, 2025. IEA. https://www.iea.org/reports/tracking-sdg7-the-energy-progress-report-2025

International Energy Agency. (2026). Tracking SDG7: The energy progress report, 2026. IEA. https://www.iea.org/reports/tracking-sdg7-the-energy-progress-report-2026

International Renewable Energy Agency. (2025). Renewable power generation costs in 2024. IRENA. https://www.irena.org/Publications/2025/Jun/Renewable-Power-Generation-Costs-in-2024

Mirjalili, S., Gandomi, A. H., Mirjalili, S. Z., Saremi, S., Faris, H., & Mirjalili, S. M. (2017). Salp Swarm Algorithm: A bio-inspired optimizer for engineering design problems. Advances in Engineering Software, 114, 163–191. https://doi.org/10.1016/j.advengsoft.2017.07.002

Modu, B., Abdullah, M. P., Alkassem, A., & Hamza, M. F. (2024). Optimal rule-based energy management and sizing of a grid-connected renewable energy microgrid with hybrid storage using Levy Flight Algorithm. Energy Nexus, 16, 100333. https://doi.org/10.1016/j.nexus.2024.100333

Mohammed, M. J., Rahmani-Fard, J., & Ridha, A. M. (2026). A comprehensive techno-economic planning framework for isolated microgrids with hybrid battery-hydrogen storage: A two-stage optimization approach. Scientific Reports. https://doi.org/10.1038/s41598-026-67945-5

Okoroafor, G. P., Oladapo, O. O., Ho, P. W. C., & Sarimuthu, C. R. (2026). Optimisation techniques for off-grid hybrid renewable energy systems with hydrogen storage: A systematic review. IET Renewable Power Generation, 20(1), e70385. https://doi.org/10.1049/rpg2.70385

Sarwar, F. A., Hernando-Gil, I., & Vechiu, I. (2024). Review of energy management systems and optimization methods for hydrogen-based hybrid building microgrids. Energy Conversion and Economics. https://doi.org/10.1049/enc2.12126

Selim, A., El-shimy, M., Amer, G., Ihoume, I., Masrur, H., & Guerrero, J. M. (2024). Hybrid off-grid energy systems optimal sizing with integrated hydrogen storage based on deterministic balance approach. Scientific Reports, 14, 6888. https://doi.org/10.1038/s41598-024-55631-3

Yadav, S., Kumar, P., & Kumar, A. (2024). Techno-economic assessment of hybrid

renewable energy system with multi energy storage system using HOMER. Energy, 297, 131231. https://doi.org/10.1016/j.energy.2024.131231